MRI and SPECT fusion for epilepsy lateralization

Kourosh Jafari-Khouzani,[*a,b] Hamid Soltanian-Zadeh,[b,c] Kost Elisevich[d]
[a]Computer Science Department, Wayne State University, Detroit, MI 48202, USA
[b]Radiology Image Analysis Lab., Henry Ford Health System, Detroit, MI 48202, USA
[c]Electrical and Computer Engineering Dept., University of Tehran, Tehran 14395, Iran
[d]Neurosurgery Dept., Henry Ford Health System, Detroit, MI 48202, USA

ABSTRACT

This paper presents a study on the SPECT images of the brain with the aim of determining the hippocampus abnormality and consequently applying timely treatment. Intensity and volume features of the hippocampus from brain MRI have been shown to be useful in detecting the abnormal hippocampus in TLE. In this study, we evaluate the intensity information of the SPECT images of the brain for the purpose of early detection of abnormal hippocampus, before the brain tissue is damaged and MRI features change. The hippocampi are segmented manually by an expert from T1-weighted MR images. The segmented regions are mapped on the corresponding SPECT images using the mutual information technique. The mean and standard deviation of the hippocampi from SPECT images are used to determine abnormal hippocampus. The experimental results show that SPECT images analyzed along with MRI generate quantitative information useful for the treatment and evaluation of epileptic patients.

Keywords: Epilepsy, SPECT, hippocampus, medical image processing

1. INTRODUCTION

Epilepsy is one of the most common disorders of the nervous system. Localization of the abnormal zones in the brain is important in the treatment of temporal lobe epilepsy (TLE). More than 20% of the epileptic patients undergo surgery when treatment with medication is ineffective. The conventional gold standard method (phase I) of evaluating an epileptic patient for surgical candidacy requires EEG exams to detect irritative zones, which is lengthy, painful, and costly. If the epileptic foci is not sufficiently localized in phase I, the patient will need to undergo phase II of the surgical evaluation, which involves implantation of electrodes intracranially and monitoring the patient for nearly two weeks.

The variations in volume and architecture of the hippocampus have been observed with some brain diseases such as schizophrenia, epilepsy, and Alzheimer.[1,2] Some attempts have been directed towards determination of hippocampus abnormalities using MR images. The proposed methods use the structural/volumetric properties, or the MR intensity variations of hippocampus. Styner et al. use a combined boundary and shape analysis based on shape descriptions to determine shape abnormalities in schizophrenia.[3]

In our early works[4,5] we used multiwavelet and wavelet texture features of the hippocampi slices from the FLAIR images of the brain to specify the candidate hippocampus for surgery in TLE. One set of features was produced by dividing the features of the right hippocampus by the corresponding features of the left hippocampus. The experimental results showed that the extracted features could help determining the abnormal hippocampus by linearly separating the left and right abnormal hippocampi. Duchesne et al.[6] employ texture analysis to classify the TLE using MR image appearance. They use a volume of interest (VOI) around the hippocampus instead of hippocampus alone. For classification of the images, models of the intensity characteristics and shape deformations of the VOI are constructed and concatenated into an appearance model for the volume. For the VOI with *n* pixels, they consider an *n*-dimensional

[*] Correspondences to: kjafari@rad.hfh.edu, hamids@rad.hfh.edu. URL: http://radiologyresearch.org

Medical Imaging 2005: Physiology, Function, and Structure from Medical Images, edited by Amir A. Amini, Armando Manduca, Proceedings of SPIE Vol. 5746
(SPIE, Bellingham, WA, 2005) · 1605-7422/05/$15 · doi: 10.1117/12.596401

space and use the principal component analysis to find the eigenvectors as orthonormal bases spanning *n*-dimensional allowable space. In this way they consider both gray-level intensities and shape deformations.

Yu et al.[7] detect abnormalities of MR images of piriform and entorhinal cortices relevant to the lithium-pilocarpine model of TLE in rats by texture analysis. They use three texture parameters derived from co-occurrence matrix to characterize structural abnormalities. Bernasconi et al.[8] study the first-order and second-order texture features to assess structural integrity of mesial temporal lobe structures (hippocampus, amygdala, and entorhinal cortex). They do a similar texture analysis work for temporopolar cortex and white matter in TLE by incorporating volumetric measurements.[9] Yu et al.[10] use first-order and second-order texture features to detect abnormality of the hippocampus in TLE. Bonilha et al. [11] use co-occurrence and run length matrices to detect hippocampal abnormalities in patients with pathologically proven hippocampal sclerosis.

Some attempts have been directed towards using the Single Photon Emission Computed Tomography (SPECT) or Positron Emission Tomography (PET) images of the brain to find the abnormal side in the TLE. Lee et al. [12] use an artificial neural network (ANN) for interpreting F-18-flurodeoxyglucose positron emission tomography (FDG PET) to find epileptogenic zones based on the diagnostic criteria and the decision rules of human experts. They use asymmetric indexes of mirrored regions to the midline for 17 cerebral regions from predefined volumes of interest on the template, as inputs of an ANN. The patient is classified to normal, left TLE, or right TLE using the ANN.

The subtraction of the ictal and interictal SPECT images can be used to find the abnormal areas of the brain. Zubal et al. [13] use the difference images of ictal and interictal SPECT, and image processing techniques to find the epileptic seizure foci in epileptic patients. Perault et al. [14] developed a tool for comparison of brain SPECT images in epilepsy, with specific emphasis on gray-level normalization. Vera et al. [15] use the ictal-interictal subtraction images co-registered to MRI to localize seizure foci in children.

The differences in the subtraction of ictal and interictal SPECT images can also be induced by noise. Baete et al. [16] use a technique to classify the clusters of voxels in thresholded subtraction images into real perfusion differences and noise-induced differences. Aubert-Broche et al. [17] propose an unsupervised voxel neighborhood based method to assist the detection of significant functional inter-hemispheric asymmetries in brain SPECT, using anatomical information from MRI. Vohra et al. [18] apply a Kernel Fisher in the statistical analysis of shape deformations to help indicate the hemispheric location of an epileptic focus.

In this paper, we use the ictal and interictal SPECT images to detect the abnormal hippocampus. We use the SPECT images to calculate mean and standard deviation of the intensities of the hippocampi pixels. To get one set of features for each patient, the features of right hippocampus are divided by the corresponding features of the left hippocampus. In the experiments we use the images of five epileptic patients. All patients had EEG records and all of them underwent resection of one of the hippocampi. The location of seizure onset as determined by the EEG methods and the postoperative outcomes were considered as the gold standard. The experimental results show that the proposed features can linearly classify the samples for this data set.

2. METHODS

The hippocampi are first segmented from the T1-weighted images by an expert. The SPECT ictal and interictal images are then registered to T1-weighted images. The produced registered ictal and interictal SPECT images are then used for feature extraction. Using the hippocampus segmentation models on SPECT images, we calculate the mean and standard deviation of the intensity values inside the hippocampi for ictal images, interictal images and their difference. The ratios of the right and left hippocampus features are calculated to create one set of features for each patient. Using the produced features and a linear classifier, the patients are classified to the right or left abnormal side. In the following subsections, the details of this method are explained.

2.1. Hippocampus Segmentation

Since the extracted features depend on the hippocampi segmentation, our collaborating neuronatomist-neurosurgeon manually segments the hippocampi from the T1-weighted images to avoid possible problems with automatic methods.

A sample of manual segmentation on the sagittal and coronal T1-weighted images of the brain is shown in Fig. 1. The SPECT images are registered to the T1-weighted images. The segmented models are then used on the registered SPECT image. Fig. 2 shows the sagittal and coronal view of ictal SPECT images of a patient with the mapped segmentation model. We use the intensity values of the registered SEPCT images for feature extraction. Since SPECT images have low spatial resolution, we do not lose much when we use the registered SPECT images instead of the original images.

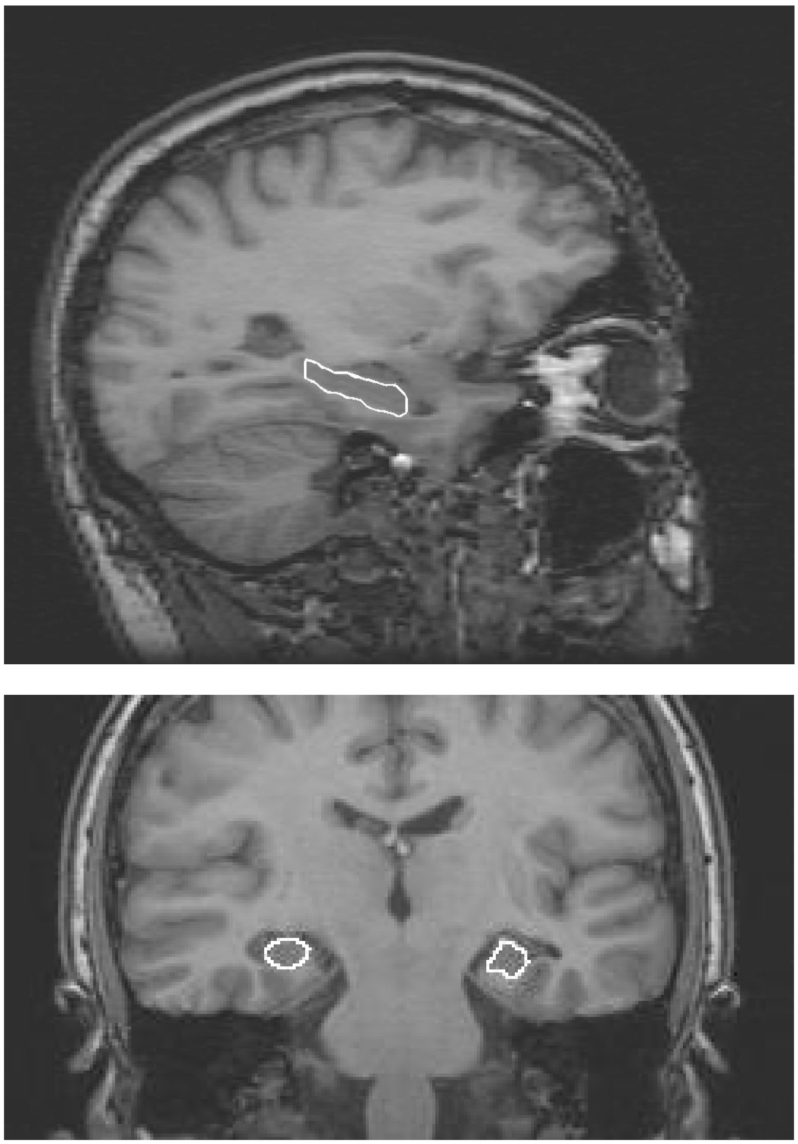

Fig. 1. Sagittal and coronal views of manual hippocampus segmentation on T1-weighted MR images.

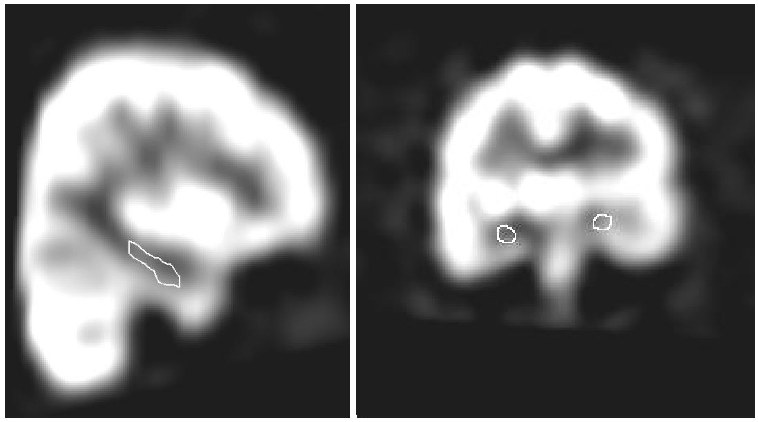

Fig. 2. Sagittal and coronal views of manual hippocampus segmentation on SPECT images.

2.2. Feature Extraction

Using the hippocampus model of T1-weighted images, we extract the mean μ and standard deviation σ of the intensity values of hippocampus in the registered SPECT images as follows:

$$\mu = \frac{1}{N}\sum_{x}\sum_{y} I(x, y)$$

$$\sigma^2 = \frac{1}{N}\sum_{x}\sum_{y}\left(I(x, y) - \mu\right)^2$$

where $I(x,y)$ shows the intensity values of the hippocampus and N is the number of pixels in the hippocampus. We calculate these features for ictal images, interictal images and their difference.

Like our previous work in reference[4], an important practical issue in extracting intensity-based features is that, SPECT images of different patients have different ranges of intensities, which may considerably affect the extracted features. As it is often the case, only one of the hippocampi is abnormal in each patient. To get one set of features for each patient, we divide the resulting features of the right hippocampus (i.e., mean and standard deviation) by the resulting features of the left hippocampus and use these ratios as the final set of features for each patient. The resulting features are called mean and standard deviation ratios, respectively.

2.3. Classification

We employ a linear classifier, which is supervised and can be easily implemented by a neural network as shown in Fig. 3. As shown, this neural network has a two-value output, which shows either left or right hippocampus is abnormal. The weighted sum of the features plus a bias is the discriminant function. To determine how effectively the classes are separated, we use the EEG phase II results as the gold standard.

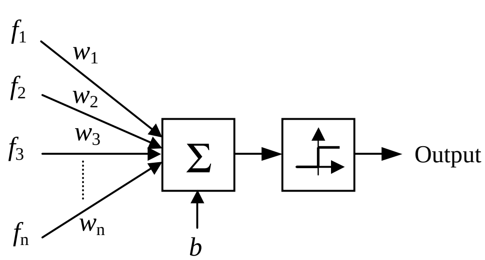

Fig. 3. The linear classifier.

3. EXPERIMENTAL RESULTS

In the experiments, we used the ictal and interictal SPECT images of five patients, one with right abnormal and four with left abnormal hippocampi. We calculated the features for each patient as described in Section 2. Fig. 4 shows the scatter plots of the extracted features for ictal and interictal SPECT images, and their difference. The “R” and “L” symbols respectively show the patients with right and left abnormal hippocampi.

As shown, the samples are linearly separable for ictal images, and the difference of ictal and interictal images. There is a better separation between left and right abnormal samples when using the features of the difference images (Fig. 4(c)). This shows that the extracted features may distinguish between the right and left abnormal hippocampi in general. From Fig. 4 it can be also observed that the standard deviation ratios create better separation between the two groups compared with the mean ratios. This may be due to existence of activities near the hippocampus areas, which creates changes in the intensity values. However, due to small size of the hippocampi, the mean values may not reflect the existence of an abnormality in the brain.

The extracted features may not be seen visually by simply looking at the images. Fig. 5 shows some T1-weighted and SPECT difference images and the location of hippocampi in them. As shown, the intensity changes in the SPECT images may not reveal the abnormality of the hippocampi (except for Fig. 5 (d), in which there is a significant change in the intensity in the right hand side of the image). However, they were shown to be linearly separable using the extracted features. This shows that the quantitative measurements may classify the hippocampi when the abnormalities are not visually detectable.

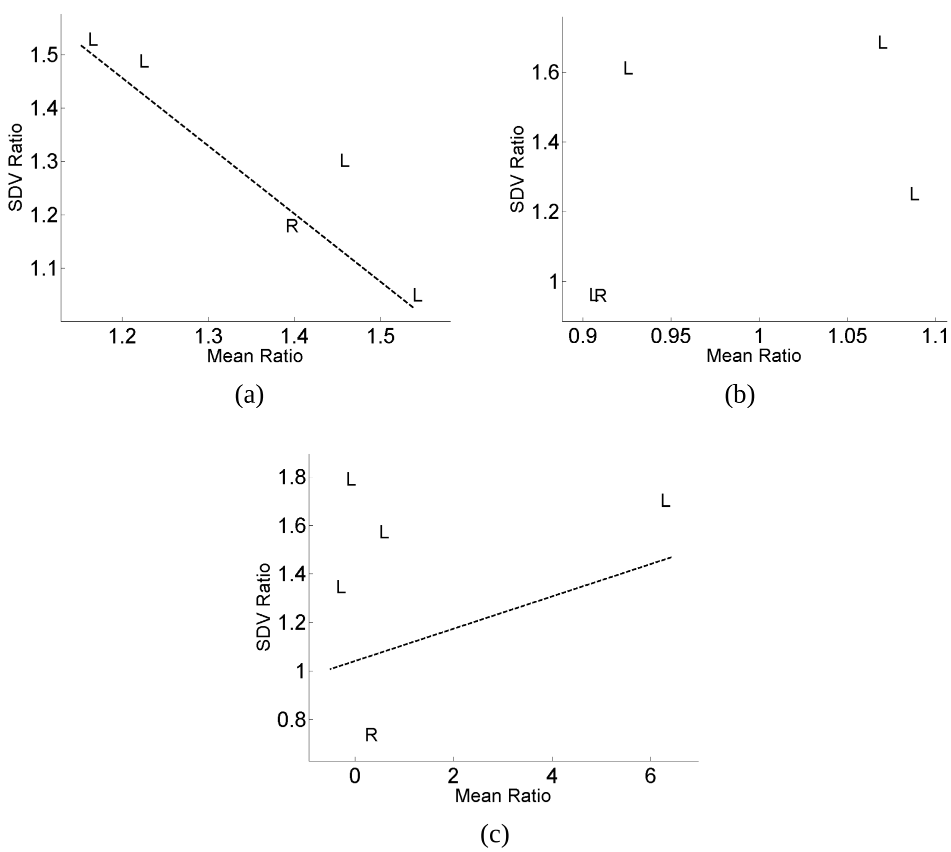

Fig. 4. Scatter plots of features for (a) ictal images, (b) interictal images, and (c) their difference. One set of features (mean and standard deviation ratios) is calculated for each patient by dividing the corresponding features of right and left hippocampi.

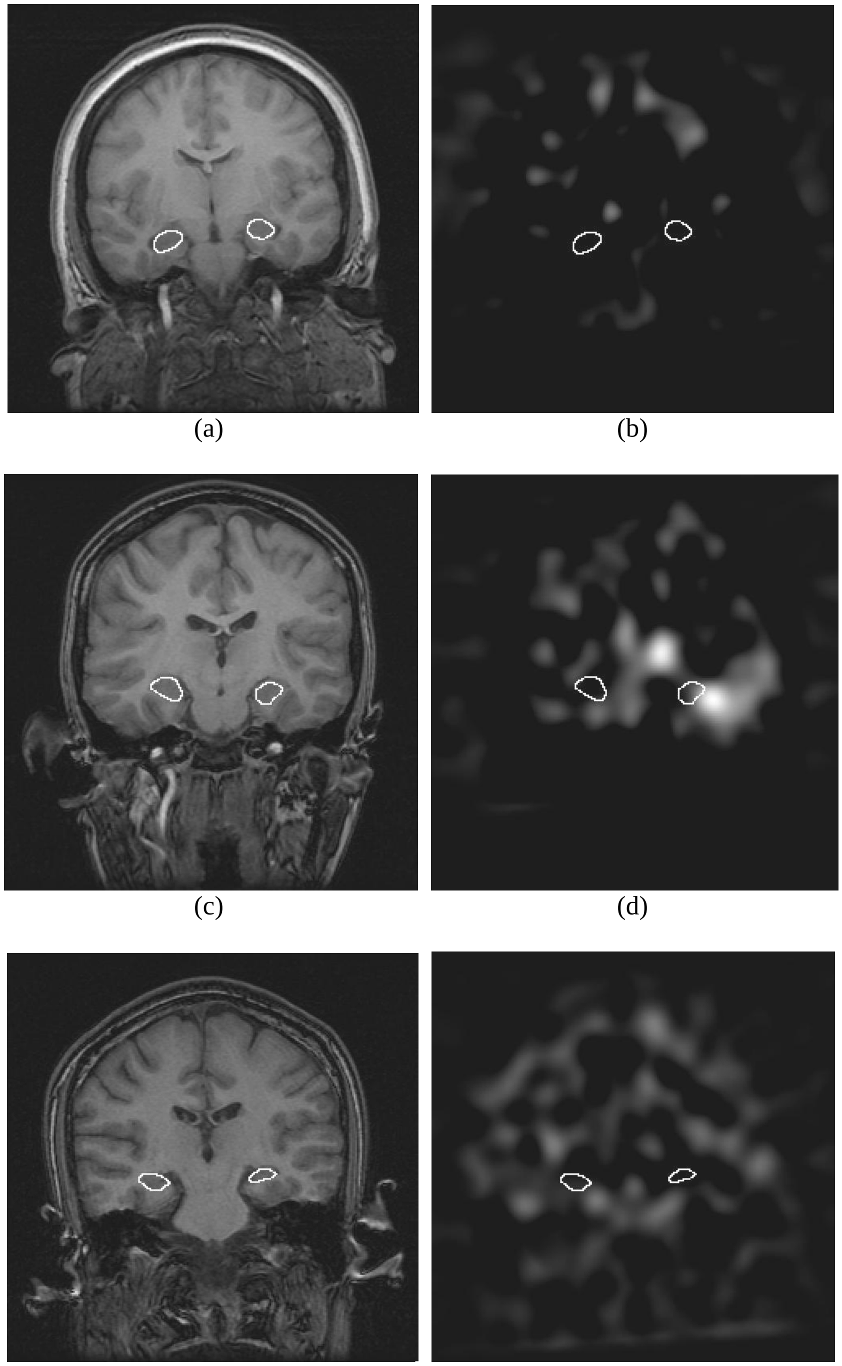

(a) (b)

(c) (d)

(e) (f)

Fig. 5. T1-weighted and ictal-interictal difference images of patients with (a) and (b) right abnormal hippocampus, (c)-(f) left abnormal hippocampus. The manual segmentations of hippocampi from T1-weighted images are mapped to the difference images. As shown, the difference images may not visually provide enough information about the abnormal side.

4. SUMMARY AND CONCLUSION

In this work, we used ictal and interictal SPECT images of five patients for feature extraction. We have focused on epileptic patients with partial seizures of presumed mesial temporal origin. All patients had EEG records and all of them underwent resection of one of the hippocampi. The location of seizure onset as determined by the EEG methods and the postoperative outcomes were considered as the gold standard. Manual segmentation results from T1-weighted images were mapped to the SPECT images. Then, using the methods explained in Sections 2, we computed a set of features and then classified them into two groups using a linear classifier. Experimental results showed that the features extracted from SPECT images might distinguish between the left and right abnormal sides. More specifically, the standard deviation ratios created better separability compared with the mean ratios. Due to the limited number of cases available for the study at this time, we are planning to evaluate the proposed methods using more cases as they become available to the project.

REFERENCES

1. C.R. Jack, R.C. Petersen, P.C. O'Brien, and E.G. Tangalos, "MR-based hippocampal volumetry in the diagnosis of Alzheimer's disease", *Neurology*, **42**, no. 1, pp. 183-188, 1992.
2. F. Cendes, F. Andermann, P. Gloor, A. Evans, M. Jones-Gotman, C. Watson, D. Melanson, A. Olivier, T. Peters, I. Lopes-Cendes, and G. Leroux, "MRI volumetric measurement of amygdala and hippocampus in temporal lobe epilepsy", *Neurology*, **43**, no. 4, pp. 719-725, 1993.
3. M. Styner, J.A. Lieberman, and G. Gerig, "Boundary and medial shape analysis of the hippocampus in schizophrenia", *Proc. 6th Int. Conf. MICCAI*, 2879, pp. 464-471, 2003.
4. K. Jafari-Khouzani, M.-R. Siadat, H. Soltanian-Zadeh, and K. Elisevich, "Texture analysis of hippocampus for epilepsy", *Proc. SPIE: Medical Imaging*, 5031, pp. 279-288, Feb. 2003.
5. K. Jafari-Khouzani, M.-R. Siadat, H. Soltanian-Zadeh, K. Elisevich, and S. Patel, "Comparison of 2D and 3D wavelet features for TLE lateralization", *Proc. SPIE: Medical Imaging*, 5369, pp. 593-601, Feb. 2004.
6. S. Duchesne, N. Bernasconi, A. Bernasconi, and D.L. Collins, "On the classification of temporal lobe epilepsy using MR image appearance", *Proc. 16th Int. Conf. on Pattern Recognition*, 1, pp. 520-523, 2002.
7. O. Yu, C. Roch, I.J. Namer, J. Chambron, and Y. Mauss, "Detection of late epilepsy by the texture analysis of MR brain images in the lithium-pilocarpine rat model", *Magnetic Resonance Imaging*, **20**, pp. 771-775, 2002.
8. N. Bernasconi, S. B. Antel, and A. Bernasconi, "Texture analysis in mesial temporal lobe epilepsy", *Proc. Int. Mag. Reson. Med.*, 11, pp. 2021-2021, 2003.
9. N. Bernasconi, S. B. Antel, T. Sankar, and A. Bernasconi, "Quantitative assessment of temporopolar cortex and white matter in temporal lobe epilepsy using volumetric MRI and texture analysis", *Proc. Int. Mag. Reson. Med.*, 11, pp. 2023-2023, 2003.
10. O. Yu, Y. Mauss, I.J. Namer, and J. Chambron, "Existence of contralateral abnormalities revealed by texture analysis in unilateral intractable hippocampal epilepsy", *Magnetic Resonance Imaging*, **19**, no. 10, pp. 1305-1310, 2001.
11. L. Bonilha, E. Kobayashi, G. Castellano, G. Coelho, E. Tinois, F. Cendes, and L.M. Li, "Texture analysis of hippocampal sclerosis", *Epilepsy*, **44**, no. 12, pp. 1546-1550, 2003.
12. J. S. Lee, D. S. Lee, S.-K. Kim, S.-K. Lee, J.-K. Chung, M. C. Lee, and K. S. Park, "Localization of epileptogenic zones in F-18 FDG brain PET of patients with temporal lobe epilepsy using artificial neural network", *IEEE Trans. Medical Imaging*, **19**, no. 4, pp. 347-355, 2000.
13. I.G. Zubal , S.S. Spencer, K. Imam, J. Seibyl, E.O. Smith, G. Wisniewski, and P.B. Hoffer P.B., "Difference images calculated from ictal and interictal technetium-99m-HMPAO SPECT scans of epilepsy", *Journal of Nuclear Medicine*, **36**, no. 4, pp. 684-689, 1995.
14. C. Perault, D. Papathanassiou, H. Wampach, P. Vera, A. Kaminska, C. Chiron, P. Peruzzi, J.-C. Liehn, "Computer-aided intrapatient comparison of brain SPECT images: the gray-level normalization issue applied to children with epilepsy", *Journal of Nuclear Medicine*, **43**, no. 6, pp. 715-724, June 2002.
15. P. Vera, I. Gardin, H. Foehrenbach, J.-L. Stievenart, A. Kaminska, C. Cieuta, A. Hollo, D. Ville, P. Plouin, O. Dulac, and C. Chiron, "Ictal-interrictal substraction TEMP images co-registered to MRI: methods and interest in partial epilepsy resistant to therapy in children", *Medecine Nucleaire*, **22**, no. 7, pp. 357-370, Nov. 1998.

16. K. Baete, J. Nuyts, W. Van paesschen, A. Maes, S. Ghoorun, P. Suetens, and P. Dupont, "Use of excess height and cluster extent in subtraction SPECT", *IEEE Trans. Nuclear Science*, **49**, no. 5, pt. 1, pp. 2332-2337, 2002.
17. B. Aubert-Broche, C. Grova, P. Jannin, I. Buvat, H. Benali, and B. Gibaud, "Detection of inter-hemispheric asymmetries of brain perfusion in SPECT", *Physics in Medicine and Biology*, **48**, no. 11, pp. 1505-1517, June 2003.
18. N. Vohra, B.C. Vemuri, A. Rangarajan, R.L. Gilmore, S.N. Roper, and C.M. Leonard, "Kernel Fisher for shape based classification in epilepsy", *Proc. 5th Int. Conf. MICCAI*, **2489**, pp. 436-443, 2002.